JOURNAL OF
Materials
CHEMISTRY

Characterization of semicrystalline titanium(IV) phosphates and their selectivity of cations and lithium isotopes

Hiroaki Takahashi,[a] Takao Oi*[a] and Morikazu Hosoe[b]

[a]*Department of Chemistry, Sophia University, 7-1 Kioicho, Chiyodaku, Tokyo, 102-8554, Japan. E-mail: t-ooi@sophia.ac.jp*
[b]*Department of Earth and Ocean Sciences, National Defense Academy, 1-10-20 Hashirimizu, Yokosuka, Kanagawa, 239-8686, Japan*

Received 3rd April 2002, Accepted 17th May 2002
First published as an Advance Article on the web 19th June 2002

A semicrystalline layered titanium phosphate (scTiOP), which showed the chemical properties of a cation exchanger, was synthesized from a mixed solution of titanyl sulfate and ammonium dihydrogenphosphate solutions under mild conditions. Based on the results of ^{31}P MAS NMR measurements, infrared measurements, thermogravimetry–differential thermal analysis, ICP atomic emission spectroscopic analysis and powder X-ray diffraction analysis, the ion exchanger was identified as $Ti_2O_3(H_2PO_4)_2\cdot 2H_2O$. Ion exchangers with varying degrees of condensation of the dihydrogenphosphate groups, and consequently having three-dimensional cross-linked structures with minutely controlled ion exchange sites, were obtained by the thermal treatment of scTiOP at different temperatures. The ion exchangers obtained by thermal treatment at temperatures from 200 to 600 °C showed a high affinity toward sodium ion among the alkali metal ions, whereas scTiOP and the ion exchanger treated at 100 °C showed no specific selectivity of any alkali metal ion. The single-stage separation factor, *S*, for the lithium isotopes was a slow increasing function of the temperature of the thermal treatment up to 600 °C, and the maximum *S* value at 25 °C was 1.028. The occurrence of a high affinity to sodium ion, the increase in *S* value and the development of a three dimensional –O–P–O– network seemed mutually correlated.

Introduction

Separation of lithium isotopes is a major concern in nuclear science and technology in connection with the future energy problem, as one of the stable isotopes of lithium, ^{6}Li, will be required for the tritium breeder blanket in deuterium–tritium fusion power reactors. Various methods for separation of the lithium isotopes have been developed. Ion exchange chromatography is certainly a candidate for a large scale production of enriched lithium isotopes. With commercially available ion exchangers as column packing materials, a value for the single-stage separation factor for lithium isotopes of up to about 1.003 has been observed at room temperature.[1] Here, the separation factor, *S*, is defined as,

$$S = \frac{\text{Amount of } ^7\text{Li in solution phase}}{\text{Amount of } ^6\text{Li in solution phase}} \times \frac{\text{amount of } ^6\text{Li in ion exchanger phase}}{\text{amount of } ^7\text{Li in ion exchanger phase}} = (^7\text{Li}/^6\text{Li})_{\text{solution}}/(^7\text{Li}/^6\text{Li})_{\text{ion exchanger}}$$

where $(^7\text{Li}/^6\text{Li})_A$ denotes the ^{7}Li/^{6}Li isotopic ratio in phase A. An *S* value of 1.003 is rather small and materials that show large lithium isotope effects have been sought for the development of lithium isotope separation processes with high performance.

It has been reported that some inorganic ion exchangers show larger lithium isotope effects, from several times to over one order of magnitude, than those of organic ion exchangers. They include manganese oxides-based ion exchangers,[2–6] niobic and tantalic acids,[7] antimonic acids[3,8,9] and could be an alternatives to organic ion exchangers.

A loose correlation has been pointed out between the lithium isotope selectivity and the alkali metal ion selectivity for inorganic ion exchangers;[3,7,8] those with high affinity toward lithium or sodium ions, from among the alkali metal ions, tend to show large lithium isotope selectivity. This indicates that the size and shape of the ion exchange sites is an important factor in determining the lithium isotope selectivity of an ion exchanger. In this context, some kinds of zirconium(IV), titanium(IV) and zirconium/titanium phosphate-based ion exchangers may be a substitute for organic ion exchangers in chromatographic lithium isotope separation processes. In previous papers,[10,11] we reported the selectivity of alkali metal ions and lithium isotopes on crystalline zirconium(IV) and zirconium(IV)–titanium(IV) phosphates with three dimensional structures. Lithium isotope selectivity on layered zirconium and titanium phosphates was also reported.[12]

In a recent preliminary paper,[13] we synthesized, from an aqueous solution containing titanium(IV) and dihydrogenphosphate ions, a semicrystalline titanium(IV) phosphate that has the properties of a cation exchanger and found that its thermally-treated products showed relatively large lithium isotope effects. It was speculated that the titanium phosphate obtained as a precipitate from the aqueous solution was dehydrated by the thermal treatment to develop a structure partially bridged by P–O–P bonds in the pyrophosphate form, which led to a relatively high lithium isotope selectivity. It was thus expected that it might be possible to control the size of the ion exchange sites and, consequently, the lithium isotope selectivity because by controlling the degree of cross-linking using the conditions of the thermal treatment, the spatial distribution of the non-bridged phosphate groups could be changed. In this paper, we report on the structural change of the semicrystalline layered titanium phosphate (scTiOP) caused by the thermal treatment and on the change in its cation and lithium isotope selectivity subsequently observed.

DOI: 10.1039/b203266j

Experimental

Preparation of the ion exchangers

To an aqueous solution of titanyl sulfate was slowly added an aqueous solution of ammonium dihydrogenphosphate at 70 °C with stirring until the P : Ti molar ratio became 1 : 1. The pH of the mixed solution was adjusted to 1 with ammonia and the solution was allowed to stand at 100 °C for 10 days with occasional shaking. The precipitate formed was filtered, washed with distilled water and air dried at room temperature. The precipitate thus treated showed ion exchange properties and is hereafter denoted as scTiOP, with "sc" meaning "semicrystalline". The precipitate was heated at different temperatures of between 100 and 800 °C for 10 h. The product at each temperature is designated as scTiOP-xxx where xxx is the temperature of the thermal treatment in °C.

Characterization

The P : Ti molar ratio in the scTiOP was determined by HF–HNO_3–HCl decomposition followed by the determination of concentrations of P and Ti in the resultant solution by ICP atomic emission spectroscopy (ICP-AES) with a Seiko Instruments SPS7700 ICP-AES spectrometer. IR spectra were recorded with a PerkinElmer 1950 IR spectrometer using the KBr pellet technique. Thermogravimetry–differential thermal analysis (TG-DTA) data were collected with a Rigaku TAS-200 TG-DTA analyzer, and identification of the gases released during TG measurements was done with an apparatus consisting of a PerkinElmer Spectrum 2000 IR spectrometer and a PerkinElmer TGA7 TG analyzer. The powder X-ray diffraction (XRD) patterns were recorded using a Rigaku RAD-IIA X-ray diffractometer with the Cu Kα radiation (λ = 1.54056 Å) in the 2θ range 5–70° at room temperature. The interlayer distance of scTiOP was determined with silicon as the internal standard at a 2θ scan rate of 1° min^{-1}. ^{31}P magic-angle spinning nuclear magnetic resonance (MAS NMR) spectra were obtained with a JEOL Lambda-300 spectrometer using an 85% aqueous phosphoric acid solution as the external standard. The concentrations of the alkali metal ions in solution were determined by flame photometry with a Daini Seikosha SAS-727 atomic absorption spectrometer, and those of the alkaline earth metal ions by ICP-AES.

The ion exchange properties of the precipitate and its thermally treated products were examined in four aspects, *i.e.*, behavior in pH titration, ion selectivity, lithium isotope selectivity and ion uptake.

The pH titration was conducted on scTiOP. 0.1 g of scTiOP was immersed in 15 cm^3 of a mixed solution of LiOH and LiCl solutions with the lithium concentration of 0.10 mol dm^{-3} under an N_2 atmosphere. After the ion exchange equilibrium was attained, the pH and lithium and phosphorus concentrations of the supernatant were measured.

To examine the alkali metal and alkaline earth metal ion selectivity, the distribution coefficient, K_d, in cm^3 g^{-1} is calculated by the formula,

$$K_d = \frac{\text{Amount of cation in 1 g solid phase}}{\text{Amount of cation in 1 cm}^3\text{ solution phase}}$$

0.1 g of the ion exchanger was placed in 10 cm^3 of NH_3–NH_4Cl buffer solution of pH 9.18 containing Li^+, Na^+, K^+, Rb^+, Cs^+, Mg^{2+}, Ca^{2+}, Sr^{2+} and Ba^{2+} ions of 1.0 mmol dm^{-3} at 25 °C for 7 days. The two phases were then separated by filtration, and concentrations of the ions in the solution phase were measured. The amount of an ion taken up into the ion exchanger phase was calculated from the concentration difference in the solution phase before and after the ion exchange equilibrium.

The lithium isotope selectivity was estimated batchwise as the S value. 0.12 g of the ion exchanger was placed in 3 cm^3 of 0.1 mol dm^{-3} lithium hydroxide solution, and the solution was maintained at 25 °C for 7 days. The ion exchanger was then separated from the solution by filtration. The lithium isotopic ratio, $^7Li/^6Li$, of the solution phase was measured by the surface ionization technique with a Finnigan Mat 261 mass spectrometer after the chemical form of the lithium was converted from hydroxide to iodide. From the experimental data in the solution phase, S was actually calculated using the following equation,

$$S = [r(1+r)C_0 - r(1+r_0)C]/[r_0(1+r)C_0 - r(1+r_0)C]$$

where C_0 and C are the lithium concentrations before and after the equilibrium, respectively, and r_0 and r are the lithium isotopic ratios before and after the equilibrium, respectively.

In the above experiment, the lithium ion uptake was also calculated from the concentration difference in the solution phase before and after the ion exchange equilibrium, and the rate of phosphate release under basic conditions was determined by measuring the concentration of phosphorus in the solution phase after the equilibrium. Similar experiments were performed for sodium starting from 0.1 mol dm^{-3} sodium hydroxide solution instead of from lithium hydroxide solution.

Results and discussion

Characterization of ion exchangers prepared

Chemical analysis showed that the P : Ti ratio of scTiOP is 0.96 : 1.0, nearly the same as that of the mother solution. The XRD pattern of scTiOP is shown in Fig. 1(a). Several broad peaks and a peak at 2θ = 8.82°, which is ascribable to the layered structure with an interlayer distance of 10.0 Å, are observed. Thus, scTiOP has a layered structure with low crystallinity. A very similar XRD pattern to that of scTiOP is reported for a semicrystalline layered titanium hydrophosphate of probable formula $Ti(OH)_2(HPO_4)\cdot H_2O$ with an interlayer distance of 10.1 Å.[14] The XRD pattern of scTiOP is also similar to that of another layered titanium phosphate, $Ti_2O_3(H_2PO_4)_2\cdot 2H_2O$, abbreviated hereafter as TiOP,[15] except that the interlayer distance of TiOP is 9.9 Å and its crystallinity is much higher than that of scTiOP. Chemical analysis and comparison

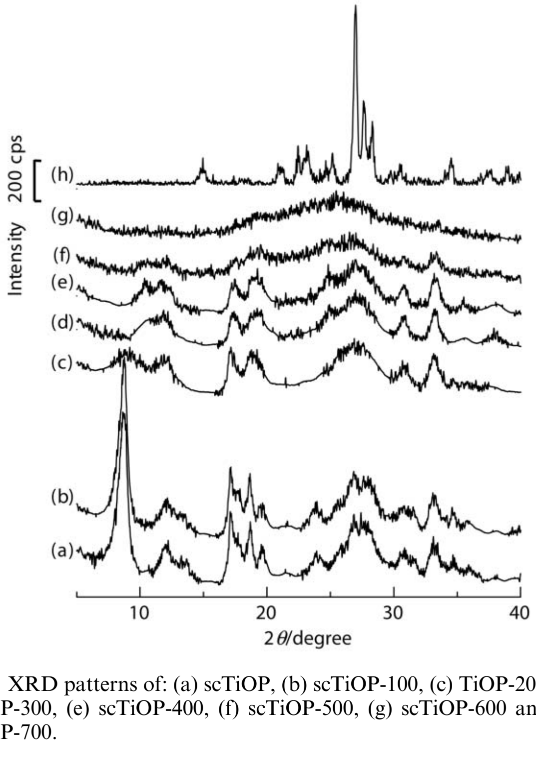

Fig. 1 XRD patterns of: (a) scTiOP, (b) scTiOP-100, (c) TiOP-200, (d) scTiOP-300, (e) scTiOP-400, (f) scTiOP-500, (g) scTiOP-600 and (h) scTiOP-700.

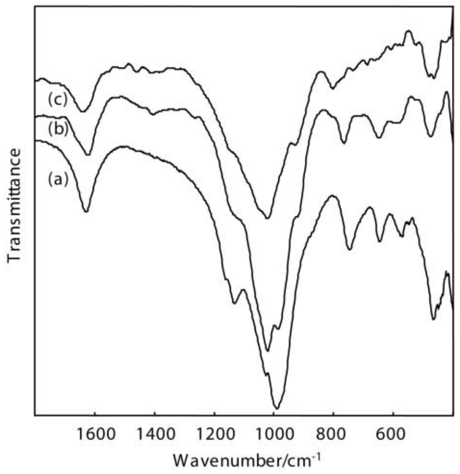

Fig. 2 IR spectra of: (a) scTiOP, (b) scTiOP-300 and (c) scTiOP-600.

of the available XRD patterns suggest that the chemical formula of scTiOP is $Ti(OH)_2(HPO_4)\cdot H_2O$ or $Ti_2O_3(H_2PO_4)_2\cdot 2H_2O$.

The IR spectrum of scTiOP is shown in Fig. 2(a). This is a typical spectrum for layered titanium phosphates. The peaks at 990, 1027 and 1131 cm^{-1} are assignable to the P–O stretching modes of the $-H_2PO_4$ group, and those at 746 and 646 cm^{-1} to Ti–O vibrational modes in the Ti–O–P matrix. Thus, the IR data support the speculation that scTiOP is of a layered structure and has $-H_2PO_4$ groups.

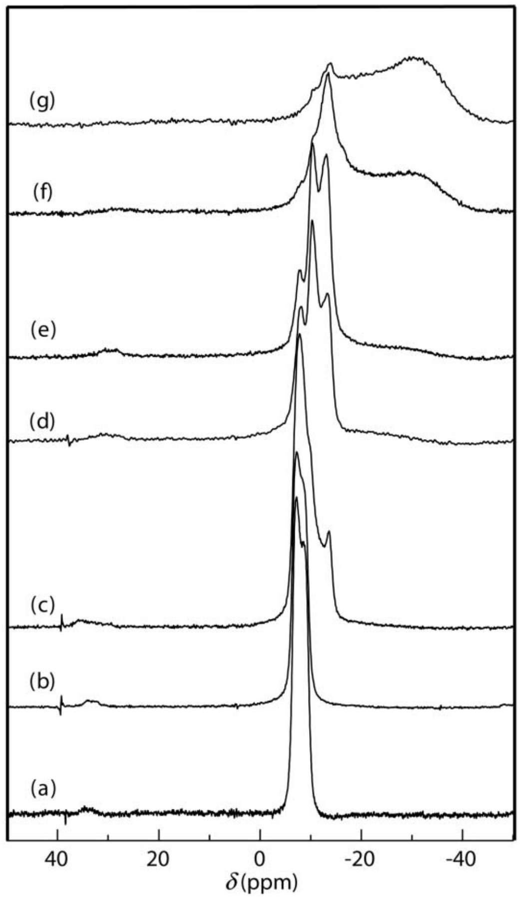

Fig. 3 ^{31}P MAS NMR spectra of: (a) scTiOP, (b) scTiOP-100, (c) TiOP-200, (d) scTiOP-300, (e) scTiOP-400, (f) scTiOP-500 and (g) scTiOP-600.

Table 1 ^{31}P NMR shifts (ppm) in titanium phosphates

Titanium phosphate	H_2PO_4	HPO_4	PO_4	Ref.
$Ti(HPO_4)_2\cdot H_2O$ (α-TiP)	—	−18.1	—	14, 15, 17
$Ti(H_2PO_4)(PO_4)\cdot 2H_2O$ (γ-TiP)	−10.6	—	−32.5	14, 15, 17
$TiO(OH)(H_2PO_4)\cdot 2H_2O$	−6.5, −8.4	—	—	17
$Ti_2O_3(H_2PO_4)_2\cdot 2H_2O$ (TiOP)	−5.3, −7.6	—	—	15

The ^{31}P MAS NMR spectrum of scTiOP is shown in Fig. 3(a). Two closely located signals are observed at −7.0 and −8.7 ppm. Several papers have previously reported ^{31}P MAS NMR data for titanium phosphates,[14–21] and Table 1 summarizes the ^{31}P NMR chemical shifts of the H_3PO_4 family in solid titanium phosphates whose chemical formulae are explicitly expressed and confirmed.[14,15,17] Consulting this table, the two signals in Fig. 3(a) are ascribed to two crystallographically inequivalent $-H_2PO_4$ groups, supporting the IR evidence that scTiOP has $-H_2PO_4$ groups as ion exchange groups and ruling out the possibility that the chemical formula of scTiOP is $Ti(OH)_2(HPO_4)\cdot H_2O$. The small discrepancies in the ^{31}P NMR chemical shifts for the $-H_2PO_4$ groups observed among our scTiOP and titanium phosphates, see Table 1, are probably due to the slight difference in hydrogen bonding in connection with the difference in crystallinity, as pointed out by Bortun *et al.*[15]

The TG curve of scTiOP is shown in Fig. 4. Weight losses of 9.6, 4.8 and 4.8 wt.% are observed between 50 and 150 °C, between 150 and 280 °C and between 280 and 600 °C, respectively, indicating that the pyrolysis of scTiOP occurs in three steps. The total weight loss amounts to 19.2 wt.% up to 600 °C. The weight loss in each step and the total weight loss observed here agree well with those of $Ti_2O_3(H_2PO_4)_2\cdot 2H_2O$ (TiOP).[15] Based on the discussion by Bortun *et al.*,[15] the weight loss in the first step is ascribable to the release of water of crystallization, and those of the second and third steps to releases of the structurally bound water associated with the condensation of the $-H_2PO_4$ groups. The pyrolytic process of scTiOP may thus be expressed as,

$$Ti_2O_3(H_2PO_4)_2\cdot 2H_2O \xrightarrow[50\text{–}150\ ^\circ C]{-2H_2O} Ti_2O_3(H_2PO_4)_2 \xrightarrow[150\text{–}280\ ^\circ C]{-H_2O}$$

$$Ti_2O_3H_2P_2O_7 \xrightarrow[280\text{–}600\ ^\circ C]{-H_2O} Ti_2O_3(PO_3)_2$$

The theoretical weight losses of the three steps and the total weight loss of this process are, 9.7, 4.8, 4.8 and 19.4 wt. %, respectively, and agree well with the experimental results. The final product of the process is $Ti_2O_3(PO_3)_2$, which also agrees with the XRD measurements in Fig. 1.

All the experimental data so far presented are consistent with the claim that the chemical formula of our scTiOP is $Ti_2O_3(H_2PO_4)_2\cdot 2H_2O$, the same as that of TiOP. The crystallinity of our scTiOP is low compared with that of the TiOP from Bortun *et al.*[15] as has already been stated. This is why we

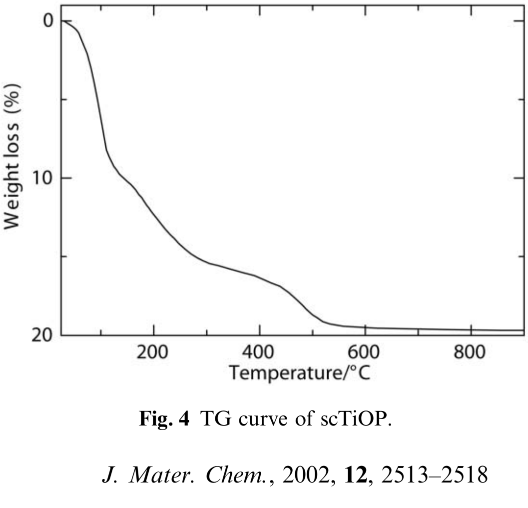

Fig. 4 TG curve of scTiOP.

have attached “sc” (meaning semicrystalline) to the TiOP to designate our titanium phosphate.

It should be noted that, although our scTiOP is the same as the TiOP of Bortun *et al.*[15] in terms of chemical formula, our scTiOP is obtained under mild experimental conditions. Our experimental temperature was 100 °C and no acid of high concentration was required, whereas the experimental temperature was 130 °C and 2 mol dm^{-3} H_3PO_4 was used in the experiment by Bortun *et al.*[15]

Some other experimental evidence supporting the scheme of the pyrolysis shown above is obtained by XRD, IR and ^{31}P MAS NMR measurements of the thermally treated products of scTiOP. The XRD patterns of the products in Fig. 1 show that the layered structure disappears when the temperature of the thermal treatment is 300 °C or higher. As the temperature increases between 300 and 600 °C, the crystallinity decreases and the product at 600 °C (scTiOP-600) is amorphous. Between 700 and 800 °C, crystalline $Ti_2O_3(PO_3)_2$ (or $(TiO)_2P_2O_7$; titanyl diphosphate) is obtained. In the IR spectra of scTiOP-300 and scTiOP-600 (Fig. 2(b) and (c)), new absorption bands appear in the 915–930 cm^{-1} and 764–800 cm^{-1} regions, which are, respectively, assignable to the symmetric and asymmetric P–O–P stretching modes of condensed phosphates.[22,23]

The ^{31}P MAS NMR spectra of the thermally treated products of scTiOP are shown in Fig. 3 and the positions and intensity ratios of the signals are summarized in Table 2. At low temperatures (100 °C and lower), two sharp signals are observed at around −7.0 and −8.7 ppm. At 200 °C, a new sharp signal appears in the higher magnetic field region of −12.9 to −13.7 ppm and the relative intensity of this signal increases with increasing temperature. At 400 °C and higher, broad signals are observed in the even higher magnetic field region of −20.7 to −30.3 ppm.

Using the ^{31}P NMR data of various titanium phosphates and oxophosphates then available, including their own, Jones *et al.*[21] discussed a correlation between connectivity and ^{31}P NMR shifts. They summarized that, as connectivity increases, an upfield shift is observed from −5.3 to −10.6 ppm for H_2PO_4 to −18.1 ppm for HPO_4 and finally to −19 to −32.5 ppm for PO_4. Based on this summarization, peaks in the regions of −7.0 to −10.4 ppm, −12.9 to −13.7 ppm and −20.7 to −30.6 ppm in Table 2 correspond to H_2PO_4, HPO_4 and PO_4, respectively. In addition, the broad breadths of the signals mean low crystallinity. Thus, the broad signals in the high field region observed for the products treated at high temperatures indicate that the condensation of dihydrogenphosphate groups is accompanied by the development of an amorphous state. This is consistent with the temperature dependence of the XRD pattern in Fig. 1.

Behavior in pH titration, ion selectivity, ion uptake and lithium isotope selectivity

The results of the pH titration are shown in Fig. 5, in which the pH of the supernatant and the lithium ion uptake are plotted against the amount of hydroxide ion added ($\mathrm{Amt_{OH}}$). A temporal decrease and a rapid increase in the lithium ion uptake are observed at around $\mathrm{Amt_{OH}}$ = 4 meq g^{-1} and at $\mathrm{Amt_{OH}}$ = 9 meq g^{-1} and larger, respectively. The shape of the lithium ion uptake–$\mathrm{Amt_{OH}}$ relation indicates that a partial decomposition of the ion exchanger by hydroxide ions in the solution phase accompanies ion exchange when $\mathrm{Amt_{OH}}$ = 3.8 meq g^{-1} or more. A similar decomposition is reported for γ-TiOP.[24] Consulting the decomposition (hydrolysis) process of γ-TiOP, that of scTiOP may be expressed as,

Table 2 ^{31}P NMR shifts and the intensity ratios in titanium phosphates prepared in this work

Ion exchanger	^{31}P NMR shift (ppm)	Intensity ratio
scTiOP	−7.0, −8.7	1 : 1
scTiOP-100	−7.1, −8.8	1 : 1
scTiOP-200	−7.8, −9.9, −13.7	10 : 10 : 3
scTiOP-300	−8.1, −10.3, −13.6	3 : 8 : 4
scTiOP-400	−7.6, −10.4, −12.9, −25.9	1 : 5 : 6 : 1
scTiOP-500	−10.4, −13.3, −20.7, −30.6	1 : 10 : 6 : 7
scTiOP-600	−13.7, −22.3, −30.3	2 : 3 : 4

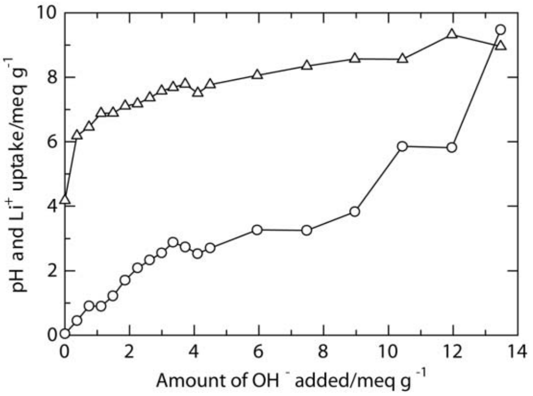

Fig. 5 Plots of lithium ion uptake (○) and pH (△) against amount of hydroxide ion added in pH titration.

$$\mathrm{Ti_2O_3(H_2PO_4)_2{\cdot}2H_2O + 2OH^- + (\mathit{n}-3)H_2O \rightarrow}$$
$$\mathrm{2TiO_2{\cdot}(\mathit{n}/2)H_2O + 2H_2PO_4^-}$$

Based on this decomposition scheme for scTiOP, the amount of decomposed scTiOP is equal to one half of the amount of phosphorus found in the supernatant. Using this relation and a theoretical ion exchange capacity for scTiOP of 10.68 meq g^{-1} estimated by reasonably assuming that its chemical formula is $Ti_2O_3(H_2PO_4)_2{\cdot}2H_2O$ and H^+ ions of dihydrogenphosphate groups alone contribute to ion exchange, the degree (%) of hydrolysis of scTiOP, D_{hyd}, and the degree (%) of ion exchange between hydrogen and lithium ions, D_{exch}, are calculated and plotted against $\mathrm{Amt_{OH}}$ in Fig. 6. The hydrolysis of scTiOP commences practically at around $\mathrm{Amt_{OH}}$ = 3.8 meq g^{-1}, and the commencement of the hydrolysis coincides with that of the temporal decrease in pH in Fig. 5. The temporal decrease in pH at around $\mathrm{Amt_{OH}}$ = 4 meq g^{-1} is thus ascribable to the consumption of hydroxide ions and the release of dihydrogenphosphate ions. D_{exch} is an increasing function of $\mathrm{Amt_{OH}}$ with a temporal decrease at around $\mathrm{Amt_{OH}}$ = 4 meq g^{-1} and reaches 99% at $\mathrm{Amt_{OH}}$ = 13.5 meq g^{-1}.

The logarithms of the distribution coefficients are plotted as functions of the temperature of the thermal treatment in Fig. 7. As for alkali metal ion selectivity, scTiOP and scTiOP-100 show no specific selectivity toward any alkali metal ion. An especially high selectivity to sodium ion is observed for the ion

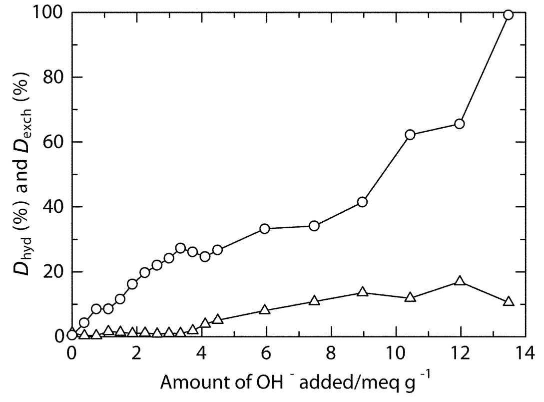

Fig. 6 Plots of degrees of ion exchange (○) and hydrolysis (△) against amount of hydroxide ion added.

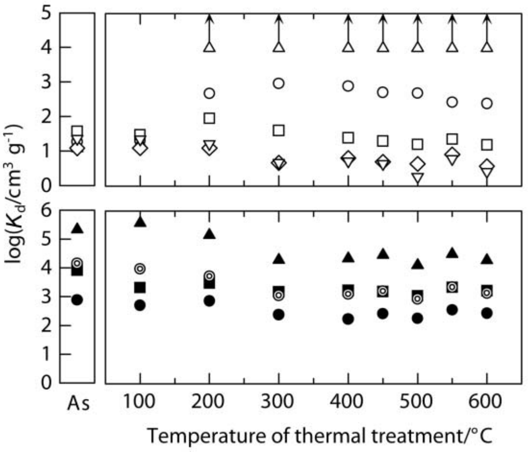

Fig. 7 Plots of distribution coefficients of Li^+ (○), Na^+ (△), K^+ (□), Rb^+ (▽), Cs^+ (◇), Mg^{2+} (●), Ca^{2+} (■), Sr^{2+} (◎) and Ba^{2+} (▲) against the temperature of thermal treatment of scTiOP. As means "as prepared" (scTiOP). The arrows mean the K_d values are over 1×10^4.

exchangers obtained by thermal treatment at 200 °C and higher temperatures; the decreasing sequence of selectivity is $Na^+ \gg Li^+ > K^+ > Rb^+ > Cs^+$. The appearance of high selectivity for the sodium ion corresponds to that of condensed dihydrogenphosphate groups at the ion exchange sites. The decreasing order of alkaline earth metal ion selectivity is $Ba^{2+} > Sr^{2+} \approx Ca^{2+} > Mg^{2+}$ on every ion exchanger and thus the selectivity for alkaline earth metal ion is independent of the temperature of the thermal treatment. The difference in selectivity between alkaline earth metal ions and alkali metal ions suggests that the ion exchange sites for the alkaline earth metal ions are different from those of the alkali metal ions. The former is not influenced by the condensation of the dihydrogenphosphate groups and the most probable candidate is the ion exchange sites on the surfaces of the powders of the ion exchangers.

The apparent lithium and sodium ion uptakes per 1 g of ion exchanger for scTiOP to scTiOP-600 are summarized in Table 3 and the data for scTiOP to scTiOP-800 are plotted against the temperature of the thermal treatment in Fig. 8. It can be seen that the apparent lithium and sodium ion uptakes are both monotonously decreasing functions of the temperature of the thermal treatment above 300 °C. This is consistent with the pyrolytic process of scTiOP shown above; the number of ion exchangeable H^+ ions decreases in going from $Ti_2O_3(H_2PO_4)_2$ to $Ti_2O_3H_2P_2O_7$ to $Ti_2O_3(PO_4)_2$. Ion exchange does not occur very noticeably on scTiOP-700 and scTiOP-800 in accordance with the appearance of the crystalline $Ti_2O_3(PO_4)_2$ phase that has no ion exchangeable H^+ ion. It can also be observed that the sodium ion uptake is larger than that of lithium ion for every ion exchanger, which is consistent with the alkali metal ion selectivity.

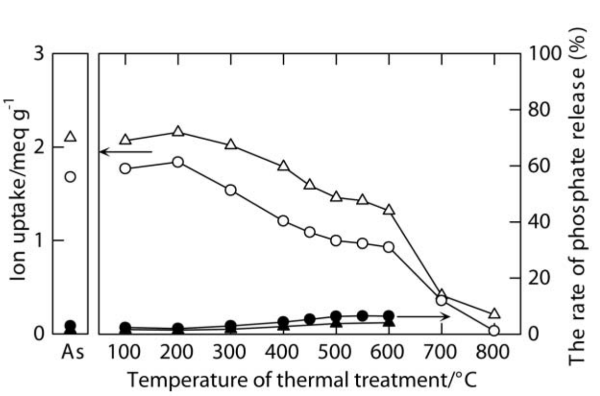

Fig. 8 Plots of Li^+ (○) and Na^+ (△) ion uptakes and the rate of phosphorus release with lithium hydroxide (●) and sodium hydroxide (▲) solutions against the temperature of thermal treatment of scTiOP. As means "as prepared" (scTiOP).

The apparent uptakes are very small both for sodium and lithium ions, compared to the theoretical capacity of 10.68 meq g^{-1}. This is partly due to the experimental setting. The solution phase contains only 0.3 mmol of lithium or sodium ion, while the solid phase is 0.12 g ion exchanger, which is equivalent to 2.5 meq ion per 1 g ion exchanger in the present experiments. Thus, only about a quarter of the theoretical ion exchange capacity can be achieved.

Table 3 Li^+ and Na^+ ion uptakes and separation factors (*S*)

Ion exchanger	Li^+ uptake/ meq g^{-1}	Na^+ uptake/ meq g^{-1}	Na^+/Li^+ uptake ratio	*S*
scTiOP	1.68	2.10	1.25	1.013
scTiOP-100	1.77	2.07	1.17	1.014
scTiOP-200	1.84	2.16	1.17	1.019
scTiOP-300	1.54	2.02	1.31	1.018
scTiOP-400	1.21	1.79	1.48	1.026
scTiOP-450	1.09	1.59	1.46	1.025
scTiOP-500	1.00	1.46	1.46	1.026
scTiOP-550	0.97	1.43	1.47	1.028
scTiOP-600	0.93	1.32	1.42	1.028

The rate of phosphate release (in %) is also plotted against the temperature of the thermal treatment in Fig. 8 and found to increase with increasing temperature, which is consistent with the temperature dependence of the apparent sodium and lithium ion uptakes.

The single-stage separation factor, *S*, for the lithium isotopes at 25 °C is summarized in the last column of Table 3. It is larger than unity, ranging from 1.013 to 1.028, for every ion exchanger examined, which means that the lighter isotope is preferentially fractionated into the ion exchanger phase like other inorganic ion exchangers so far investigated.[2–12] In the present experimental setting, the ion exchangers are immersed in LiOH solutions. This means that the anionic species in the solution phase are hydroxide and phosphate (and hydrogenphosphate) ions at equilibria and the molar ratio of the two ion varies from batch to batch. We have already shown that the kind of counter-ion in the solution phase has only a small effect on the *S* values in ion exchange chromatographic systems.[1] The value of *S* minus unity ($S - 1$) varies only by 1×10^{-4} with the change in the kind of counter-ion in the solution phase at 25 °C, while the variation in $S - 1$ observed in this study is of the order of 10^{-3}. The variation in *S* in Table 3 is thus ascribable in most part to the ion exchanger phase.

The value of *S* is plotted against the temperature of the thermal treatment in Fig. 9 and was found to be a slow increasing function of the temperature up to 600 °C. It is 1.013–1.014 for scTiOP and scTiOP-100 that show no specific selectivity for alkali metal ions; 1.018–1.019 for scTiOP-200

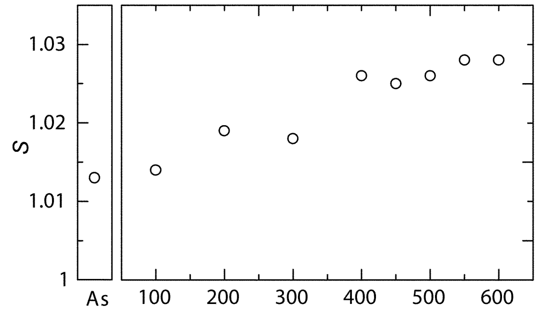

Fig. 9 Plot of single-stage separation factor for the lithium isotopes against the temperature of thermal treatment of scTiOP. As means "as prepared" (scTiOP).

Table 4 Comparison of S values for various inorganic ion exchangers under basic conditions at 25 °C

Ion exchanger	Ion selectivity	Maximum S	Ref.
Manganese oxide-based ion exchanger	Li^+	1.016	2–6
Cubic antimonic acid	Na^+	1.024	3
Monoclinic antimonic acid	Li^+	1.020	9
$HZr_2(PO_4)_3$	Li^+ and Na^+	1.019	10
$HTi_{0.5}Zr_{1.5}(PO_4)_3$	Li^+ and Na^+	1.003	11
scTiOP	Na^+	1.028	This work

and scTiOP-300 for which formation of condensed dihydrogenphosphate groups and high selectivity of the sodium ion are observed; and 1.025–1.028 for the ion exchangers treated at 400 °C and higher temperatures for which the condensation of dihydrogenphosphate groups is further developed. Thus, the value of S seems to increase with the increasing degree of condensation of the dihydrogenphosphate groups.

As shown in Table 3, the S value is 1.025–1.028 when the Na^+/Li^+ uptake ratio is 1.42 or more and is larger when the uptake ratio is 1.31 or less. This indicates that the S value is larger when the ion exchange sites show a higher affinity toward the sodium ion.

The maximum S value of 1.028 observed under highly basic conditions in this work was compared with the S values of other inorganic ion exchangers under similar conditions and the data are summarized in Table 4. As can be seen, the S value for the scTiOP is the largest, indicating that it could be a candidate for a substitute for the organic ion exchangers in chromatographic lithium isotope separation processes operating in basic solution conditions.

Conclusion

To summarize, we make the following statements:

(1) A semicrystalline layered titanium phosphate (scTiOP) was synthesized under mild conditions and was identified as $Ti_2O_3(H_2PO_4)_2{\cdot}2H_2O$. It behaved as a cation exchanger. No affinity toward a specific ion among alkali metal ions was observed. For lithium isotopes, it preferentially adsorbed ^6Li and the single-stage separation factor was 1.013 at 25 °C.

(2) Materials obtained by the thermal treatment of $Ti_2O_3(H_2PO_4)_2{\cdot}2H_2O$ at temperatures of 100 to 600 °C were also cation exchangers. The ion exchangers obtained between 200 and 600 °C showed high affinity toward sodium ion from among the alkali metal ions, whereas those obtained below 200 °C showed no specific selectivity for any alkali metal ion. The value of the separation factor for the lithium isotopes at 25 °C gradually increased with increasing temperature of the thermal treatment up to 600 °C and the maximum was 1.028. Occurrence of a high affinity toward the sodium ion and the increase in S value with increasing temperature of the thermal treatment seemed to be correlated with the development of a three-dimensional –O–P–O– network within the ion exchangers.

References

1 T. Oi, K. Kawada, M. Hosoe and H. Kakihana, *Sep. Sci. Technol.*, 1991, **26**, 1353.
2 T. Oi and A. Takiguchi, *Bull. Soc. Sea Water Sci., Jpn.*, 1993, **47**, 67, (in Japanese).
3 K. Ooi, Q. Feng, H. Kanoh, T. Hirotsu and T. Oi, *Sep. Sci. Technol.*, 1995, **30**, 3761.
4 H. Ogino and T. Oi, *Sep. Sci. Technol.*, 1996, **31**, 1215.
5 N. Izawa and T. Oi, *J. Mater. Sci.*, 1997, **32**, 675.
6 T. Takeuchi, T. Oi and H. Hosoe, *Sep. Sci. Technol.*, 1999, **34**, 545.
7 Y. Inoue, Y. Kanzaki and M. Abe, *J. Nucl. Sci. Technol.*, 1996, **33**, 671.
8 T. Oi, K. Shimizu, T. Tayama, M. Matsuno and M. Hosoe, *Sep. Sci. Technol.*, 1999, **34**, 805.
9 T. Oi, M. Endoh, M. Narimoto and M. Hosoe, *J. Mater. Sci.*, 2000, **35**, 509.
10 T. Oi, Y. Uchiyama, M. Hosoe and K. Itoh, *J. Nucl. Sci. Technol.*, 1999, **36**, 1064.
11 H. Takahashi and T. Oi, *J. Mater. Sci.*, 2001, **36**, 1621.
12 Y. Makita, H. Kanoh, T. Hirotsu and K. Ooi, *Chem. Lett.*, 1998, 77.
13 Y. Uchiyama, H. Takahashi, T. Oi and M. Hosoe, *J. Nucl. Sci. Technol.*, 2001, **38**, 85.
14 A. I. Bortun, E. Jaimez, R. Llavona, J. R. García and J. Rodríguez, *Mater. Res. Bull.*, 1995, **30**, 413.
15 A. I. Bortun, L. Bortun, A. Clearfield, M. A. Villa-García and J. Rodríguez, *J. Mater. Res.*, 1996, **11**, 2490.
16 M. J. Hudson, A. D. Workman and R. J. W. Adams, *Solid State Ionics*, 1991, **46**, 159.
17 Y. J. Li and M. S. Whittingham, *Solid State Ionics*, 1993, **63**, 391.
18 J. Soria, J. E. Iglesias and J. Sanz, *J. Chem. Soc., Faraday Trans.*, 1993, **89**, 2515.
19 C. Schmutz, P. Barboux, F. Ribot, F. Taulelle, M. Verdaguer and C. Fernandez-Lorenzo, *J. Non-Cryst. Solids*, 1994, **170**, 250.
20 E. Jaimez, A. Bortun, G. B. Hix, J. R. García, J. Rodríguez and R. C. Slade, *J. Chem. Soc., Dalton Trans.*, 1996, 2285.
21 D. J. Jones, G. Aptel, M. Brandhorst, M. Jaquin, J. Jiménez-Jiménez, A. Jiménez-López, P. Maireles-Torres, I. Piwonski, E. Rodríguez-Castellón, J. Zajac and J. Rozière, *J. Mater. Chem.*, 2000, **10**, 1957.
22 E. Steger and G. Leukrot, *Z. Anorg. Allg. Chem.*, 1960, **303**, 169.
23 D. E. C. Corbridge, M. Crayson and E. J. Griffith, in *Topics in Phosphorus Chemistry, Vol. 3*, ed. M. Grayson and E. J. Griffith, Interscience, New York, 1966.
24 E. González, R. Llavona, J. R. García and J. Rodríguez, *J. Chem. Soc., Dalton Trans.*, 1989, 829.